

SUPPLEMENTARY INFORMATION

S1. Emergence of Mn^{2+} in LSMO films and influence on XLD and XMCD spectra

The presence of this Mn^{2+} component in XAS spectra was already studied in refs.[1,2,3,4,5] and, although a clear origin could not be attributed, the presence of oxygen vacancies and the effect of reducing agents in the atmosphere were proposed as responsible of the observed Mn reduction at the surface of the films

Strain dependence of Mn^{2+} formation

As shown in the main text, a strong Mn^{2+} contribution was found in the XAS spectra of LSMO samples, here plotted in **Fig. S1(a)** as a function of c/a ratio. While the origin of the high intensity of Mn^{2+} related peaks for these samples could not be discerned, although probably related to aging effects [2], the relative intensity of peaks at 640 eV (attributed to Mn^{2+}) and 642 eV ($Mn^{3+/4+}$), was found to clearly decrease for increasing c/a ratio (**Fig. S1(b)**). It is found that, increased in-plane lattice parameter of the films is correlated with larger content of Mn^{2+} (inset in **Fig. S1(b)**).

Therefore, although more experiments are required to clearly discern the factors governing the presence of Mn^{2+} at the surface of manganite thin films, our experiments show that films under a tensile lattice strain tend to show an increased Mn^{2+} content.

This observation could be explained by increased oxygen vacancy content at the surface of tensile strained films that would help to expand the manganite lattice and hence to minimize the elastic energy. It could also be proposed a different reducing mechanism in which the reduction of Mn is favoured by the increased lattice parameter, allowing for the formation of larger Mn^{n+} cations. In this respect, Mn^{2+} is 30% larger than Mn^{3+} , thus increased lattice parameter could favour the appearance of Mn^{2+} . As it was stated in ref.[5], the energy needed to displace surrounding oxygen atoms at the surface is much smaller than in the bulk, enabling the creation of Mn^{2+} at the surface of the films.

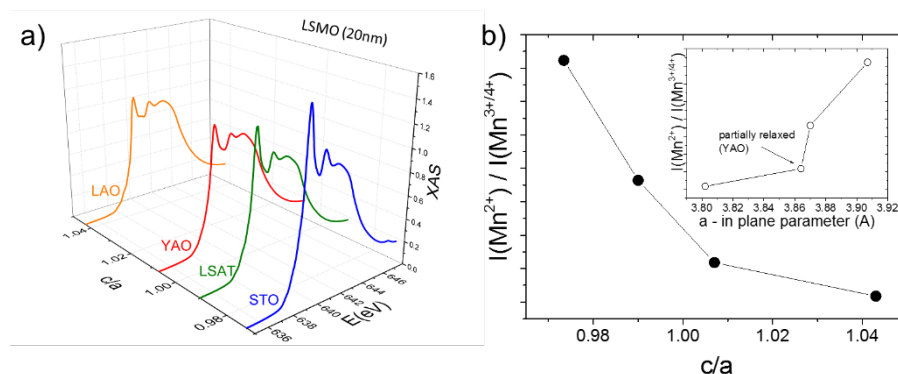


Figure S1. Mn-L₃ XAS spectra of LSMO samples as a function of c/a ratio (a); Ratio between XAS intensities at 640 eV and 642 eV, as a function of c/a (b); inset: same ratio of intensities as a function of in-plane lattice parameter of the films

Contribution of Mn^{2+} sites to linear and circular dichroic signals

The presence of Mn^{2+} at surfaces can profoundly modify the atomic environment [6] and the magnetic interactions [7]. In order to study the influence of Mn^{2+} in these characteristics we measured two similar LSMO samples (grown with the same conditions, on the same substrates) with large difference in the Mn^{2+} content at the surface (probably due to the different age of the samples). We denominated these samples: sample A (showing Mn^{2+}) and sample B (not showing Mn^{2+}).

In panel (a) of **Fig. S2** the clear difference between both samples in the XAS spectrum is shown. Red curve in the figure shows the difference between XAS spectra, clearly resembling a Mn^{2+} spectrum, as shown in the main text. The XLD signal taken at 300K (above samples T_C) in grazing incidence is shown in panel (b). While the XLD signal is identical in L_2 edge, as expected (Mn^{2+} is not a Jahn-Teller ion), a visible difference is observed in the low energy region of L_3 edge. The XLD signal can therefore be affected in this energy region by the presence of Mn^{2+} , probably due to induced artefacts in the spectra subtraction (e.g. by a time dependent increase in the Mn^{2+} content induced by x-ray irradiation). The almost perfect matching of the rest of the spectrum, however, evidences a minor contribution of Mn^{2+} to the XLD and can be safely used for comparison between samples with different Mn^{2+} content.

The magnetic contribution to low temperature dichroism is studied in panel (c) of **Fig. S2**: A clear XMCD signal (here measured at 2K under 2T applied magnetic field) attributed to Mn^{2+} is observed. By applying sum rules to both samples (considering equal number of holes $n_h = 3.5$), a relatively minor difference in m_s values ($\approx 0.3\mu_B$) is obtained, thus showing a minor effect as compared to the bulk strain-related magnetic signal observed in these samples. Moreover, the XMCD difference spectra (red line in Fig. S2(c)) can be used to subtract the Mn^{2+} contribution to XMCD signal in the rest of the samples measured, as indicated in the main text.

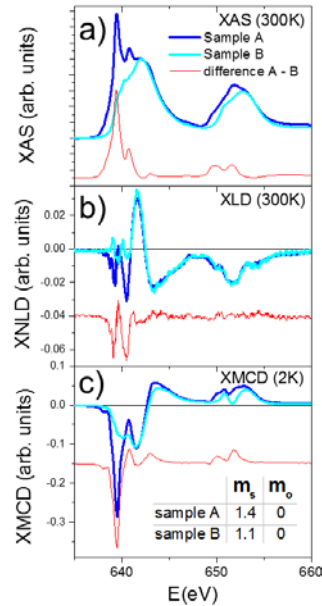


Figure S2. Room temperature XAS (a) and XLD (b) and low temperature (2K) XMCD (c) spectra of LSMO samples grown on STO: blue curve corresponds to sample A (Mn reduced sample), cyan curve corresponds to sample B (non-reduced sample) and red curve corresponds to spectra difference between them. Inset of panel c: calculated spin and orbital magnetic moments for both samples.

Annealing treatment for Mn reoxidation

A test sample ($\text{La}_{0.7}\text{Sr}_{0.3}\text{MnO}_3$ (17nm) on LAO) deposited under the same conditions as LSMO samples shown in the main text, was used to prove the effectiveness of an annealing process in reoxidating the surface of the samples. As observed in **Fig. S3(a)** (black curve), the sample showed an initial large content of Mn^{2+} , as evidenced by intense peak at 640 eV. After an annealing process with oxygen pressure $p(\text{O}_2) = 10^{-3}$ mbar, at a temperature $T = 500$ °C during 1 hour, the sample spectra showed quite reduced intensity in the XAS spectra at the low energy region of L_3 (red curve), clearly signalling an oxidation process removing the initial Mn^{2+} content and restoring the initial $\text{Mn}^{3+/4+}$ valence state. The difference spectrum, also plotted in

the figure shows the relevant decrease of the Mn^{2+} contribution to the final spectrum after annealing.

It is important to notice as well the insignificant influence of annealing process in the XLD spectra (**Fig. S3(b)**), demonstrating the null contribution of Mn^{2+} to XLD, as expected. The efficiency of this oxygenation process attests for a Mn reduction caused by oxygen vacancies at the surface of the films. As the oxygen content is restored, by means of the annealing process, Mn valence is also restored. Still, more study is necessary to explore the effects of annealing processes in thin film samples, as other phenomena like cation segregation can modify the stoichiometry and homogeneity of the samples.

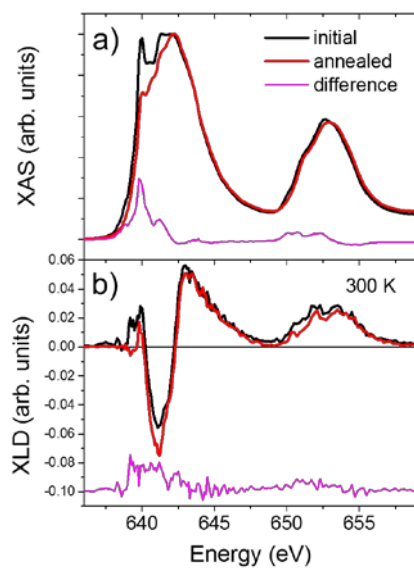


Figure S3. XAS (a) and XLD (b) spectra of LAO// $\text{La}_{0.7}\text{Sr}_{0.3}\text{MnO}_3$ sample before (black) and after (red) annealing process; the difference between both spectra is also shown (magenta).

S2. Area under XLD evaluated in different energy regions

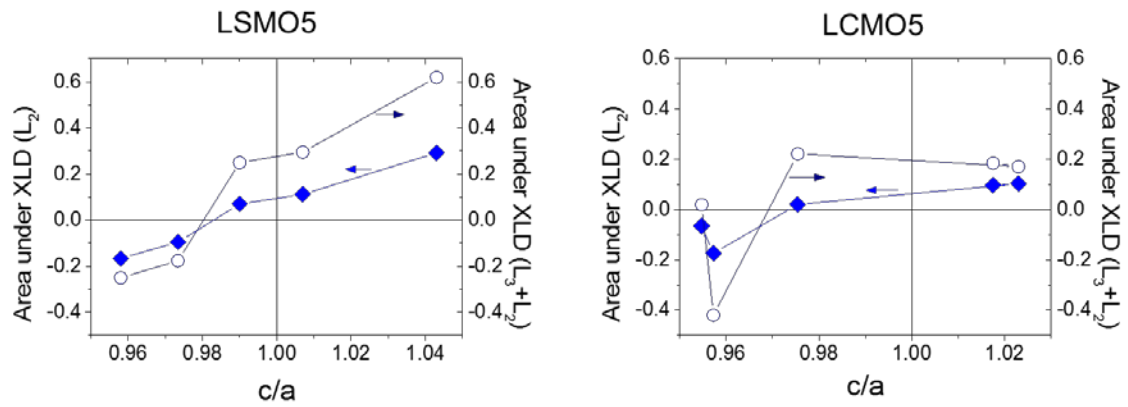


Figure S4. Integrated area under XLD as a function of c/a ratio for LSMO (left) and LCMO (right) films. Left axis and solid symbols correspond to the integrated area in the energy interval corresponding to L_2 edge, while right axis and empty symbols correspond to the area under L_2+L_3 edges.

S2. XMLD spectra of LSMO films at normal incidence

The spin alignment explored via XMLD measurements can be further checked by measuring the linear dichroic signal in normal incidence. In this geometry, no orbital contribution needs to be subtracted, as no orbital anisotropy is probed in normal incidence (same orbitals are explored for both linear polarizations), and spins with AF axis perpendicular to the sample surface do not give any dichroic signal. In **Fig.S5** we show the linear dichroism measured at 5 K in normal incidence geometry with a magnetic field ($B=2$ T) applied in the direction of the beam. The x-ray polarization vectors were parallel to sample [100] and [010] crystallographic directions. Samples on YAO and LAO show a negligible XMLD signal, which confirms the c-axis AF spin alignment. On the other hand, a clear XMLD signal is observed for sample on DSO, pointing to a preferential in-plane AF orientation that could be caused by the orthorhombic distortion existing in this substrate. Sample on STO however, does not show a clear shape of the XMLD, indicating a random in-plane direction of the AF domains.

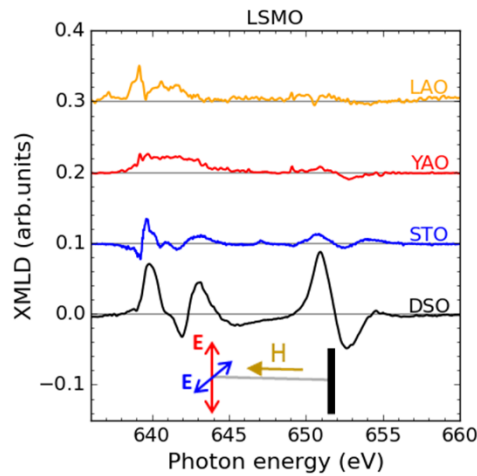


Figure S5. XMLD spectra of LSMO films, measured at 5 K with x-rays impinging in normal incidence with a 2T magnetic field was applied in the same normal direction, as sketched in the figure

¹ M. de Jong, I. Bergenti, V. Dediu, M. Fahlman, M. Marsi, and C. Taliani, *Phys. Rev. B* **71**, 014434 (2005).

² S. Valencia, A. Gaupp, W. Gudat, L. Abad, L. Balcells, A. Cavallaro, B. Martínez, and F. Palomares, *Phys. Rev. B* **73**, 104402 (2006).

³ S. Valencia, A. Gaupp, W. Gudat, L. Abad, L. Balcells, and B. Martínez, *Phys. Rev. B*, **75**, 184431 (2007).

⁴ S. Picozzi, C. Ma, Z. Yang, R. Bertacco, M. Cantoni, A. Cattoni, D. Petti, S. Brivio, and F. Ciccacci, *Phys. Rev. B*, **75**, 094418, (2007).

⁵ M. de Jong, I. Bergenti, W. Osikowicz, R. Friedlein, V. Dediu, C. Taliani, and W. Salaneck, *Phys. Rev. B*, **73**, 052403, (2006).

⁶ A. Galdi, C. Aruta, P. Orgiani, N. B. Brookes, G. Ghiringhelli, M. Moretti Sala, R. V. K. Mangalam, W. Prellier, U. Lüders, and L. Maritato, *Phys. Rev. B*, **83**, 064418 (2011).

⁷ J. J. Peng, C. Song, B. Cui, F. Li, H. J. Mao, Y. Y. Wang, G. Y. Wang, and F. Pan, *Phys. Rev. B*, **89**, 165129 (2014).